

UC San Diego

UC San Diego Previously Published Works

Title

Enzymatic Interconversion of Isomorphous Fluorescent Nucleosides: Adenosine Deaminase Transforms an Adenosine Analogue into an Inosine Analogue

Permalink

<https://escholarship.org/uc/item/3q1754vf>

Journal

Angewandte Chemie International Edition, 52(52)

ISSN

1433-7851

Authors

Sinkeldam, Renatus W
McCoy, Lisa S
Shin, Dongwon
[et al.](#)

Publication Date

2013-12-23

DOI

10.1002/anie.201307064

Peer reviewed

Published in final edited form as:

Angew Chem Int Ed Engl. 2013 December 23; 52(52): 14026–14030. doi:10.1002/anie.201307064.

Enzymatic Interconversion of Isomorphic Fluorescent Nucleosides: Adenosine Deaminase Transforms thA to thI, Two Distinct Fluorophores

Renatus W. Sinkeldam, Lisa S. McCoy, Dongwon Shin, and Yitzhak Tor*

Chemistry and Biochemistry University of California, San Diego 9500 Gilman Drive, La Jolla, CA 92093-0358, USA

Abstract

Adenosine deaminase, a major enzyme involved in purine metabolism, converts an isomorphic fluorescent analogue of adenosine (thA) to an isomorphic inosine analogue (thI), which possesses distinct spectral features, allowing one to monitor the enzyme-catalyzed reaction and its inhibition in real time. The utility of this sensitive fluorescently-monitored transformation for the high throughput detection and analysis of ADA inhibitors is demonstrated.

Keywords

Adenosine deamination; high-throughput screening; fluorescence; kinetics; nucleosides

The lack of practically useful emission for the native nucleosides A, C, G and U(T)^[1] prompted the development of fluorescent nucleosides surrogates.^[2] Such emissive analogs, in conjunction with versatile and sensitive fluorescence spectroscopy techniques,^[3] have shown to be of great value in the biophysical study of nucleic acids. Among the various classes of fluorescent nucleosides there are the isomorphic fluorescent nucleosides, characterized by an astute electronic and structural resemblance to the native nucleosides.^[2f, 4] Incorporation of such fluorescent probes is typically associated with minimal pairing, stacking and higher structural perturbation.^[2f, 4] While of great value within the context of oligomeric structures and their biophysical applications, much less is known about the function of such emissive analogs in the “protein world”, where nucleosides and nucleotides intricately interact with enzymes.^[5]

In contrast to the use of fluorogenic enzyme substrates and fluorophore precursors^[6] as well as the enzymatic unmasking or uncaging of established fluorophores for biochemical assays or imaging applications,^[7] no examples exist, to our knowledge, where isomorphic fluorescent nucleosides are transformed in enzymatically catalyzed reactions to form new and distinct fluorophores. This is likely due to the substrate specificity of many of the enzymes responsible for metabolizing and utilizing such key nucleoside and nucleotide cellular components.^[8] Here we investigate the utility of thA (**1**) a new emissive adenosine analogs and a member of our fluorescent RNA alphabet,^[9] for monitoring a catabolically important deamination reaction (Figure 1a), catalyzed by adenosine deaminase (ADA).^[10] The underlying hypothesis is that due to its similarity to adenosine, its natural counterpart, thA will be transformed to thI by ADA (Figure 1b). As thA is emissive, thI is

*Fax: (+1) 858-534-0202 ytor@ucsd.edu Homepage: <http://torgroup.ucsd.edu>.

Supporting information for this article is available on the WWW under <http://www.angewandte.org> or from the author.

likely to be fluorescent as well, yet their electronic differences are expected to render the two chromophores distinct. This, in principle, should allow one to monitor the progression of the deamination reaction in real time using fluorescence spectroscopy, an impossible task with the natural nucleobases. If successful, this can provide a new method for exploring and identifying inhibitors of ADA, small molecules of clinical utility as chemotherapeutic agents.^[11] Here we demonstrate the ability of ADA, a chief purine metabolism enzyme with both biochemical and therapeutic significance,^[11] to convert thA to thI with steady-state and kinetic analysis using absorption and emission spectroscopy. We also demonstrate the utility of this sensitive fluorescently-monitored transformation for the real-time detection of ADA inhibitors.

To be able to analytically and photophysically verify thI as the product of the enzymatic deamination of thA, thI was independently synthesized (Scheme 1).^[9] Briefly, the syntheses of thA (**1**) and thI (**2**) start from thiophene **3** which was reacted with β -D-ribofuranose 1-acetate 2,4,5-tribenzoate in the presence of SnCl₄ to give intermediate **4** as a mixture of α - and β -anomers. A subsequent tandem hydrolysis-annulation reaction furnished the protected nucleoside **5**. Following thionylation and anomer resolution, the protected nucleoside **6** was obtained as the β -anomer exclusively. A final deprotection provided thA (**1**).^[9] Conveniently, deprotection of intermediate **5** followed by anomer resolution gave thI (**2**) (Scheme 1). Starting from **3**, thA (**1**) and thI (**2**) were synthesized in an overall yield of 4.6 % and 10.7 %, respectively. X-ray crystallography unequivocally shows their correct anomeric configuration. Overlaying their crystal structures with the reported structures of their natural counterparts A^[12] and I^[13], respectively, illustrates the truly isomorphous nature of thA (**1**) and thI (**2**) (Figure 2 and S1.1 in SI).^[14] Importantly, thA (**1**) adopts an *anti*-conformation having *N*-ribose (3'-*endo*) puckering, conformational features known to be preferred by ADA.^[15]

To ensure that the photophysical characteristics of thA (**1**) and thI (**2**) are distinguishable, binary mixtures containing different ratios of the two nucleosides were examined by absorption and fluorescence spectroscopy in phosphate buffer at pH 7.4, conditions commonly used for enzymatic deamination reactions (Figure 3a). The overlaid absorption spectra of the mixtures show a distinct hypsochromic shift of the absorption maximum from that of thA (**1**) at 339 nm to that of thI (**2**) at 315 nm with a concomitant reduction in the optical density at the lower energy transition > 300 nm (Table 1). Upon excitation at 318 nm, their isosbestic point, the recorded emission spectra also present a blue shift from 410 nm, the emission maximum of thA, to 391 nm, the emission maximum of thI. In contrast to the lower optical density, the increasing thI concentration results in an increase of the emission intensity, illustrating the higher fluorescent quantum yield for thI (**2**) compared to that of thA (**1**).

To gain insight into the spectral changes, two correlation plots have been constructed (Figures 3b and 3c). Both the shift in absorption maximum and the drop in optical density show a nearly linear dependence on the thA/thI ratio (Figure 3b). Interestingly, both the emission wavelength and intensity respond linearly to an increasing thI concentration in binary mixtures with thA (Figure 3c). Clearly, absorption as well as emission spectroscopy reveal significant spectral changes suitable to study the enzymatic conversion of thA (**1**) to thI (**2**).

To investigate thA (**1**) as a substrate surrogate for adenosine in ADA-mediated deamination reactions, absorption and emission were measured before and after its reaction with ADA (Figure S2.2).^[14] The spectra obtained after the enzymatic treatment perfectly resemble the spectral characteristics of thI (**2**) (Figure 3).^[14] A control experiment using a fresh solution of thI (**2**) mixed with ADA, established that the presence of the protein does not immediately

affect the spectral properties of the emissive nucleoside (Figure S2.2).^[14] Next, the enzymatic conversion of thA (**1**) to thI (**2**) was followed in real-time using absorption as well as fluorescence spectroscopy. Absorption changes were followed at 339 nm, the $\lambda_{\text{abs.max}}$ of thI, and emission changes were followed at 391 nm, the $\lambda_{\text{em.max}}$ of thI, upon excitation at 318 nm, their isosbestic point (Figure 3d). As expected, the absorption spectra show a decrease (or an “OFF” signal) in the optical density upon conversion of thA (**1**) to thI (**2**). By exploiting thI's higher fluorescence intensity compared to thA to follow the enzymatic conversion, an intensification of the emission, or “ON” signal, is obtained. Absorption and emission spectra taken in the absence of ADA indicated that there is no conversion without the enzyme under the experimental conditions used.^[14] LC-MS analysis unequivocally confirms the enzymatic deamination of thA (**1**) and the identity of the deamination product as thI (**2**) (Figure S3.1).^[14] ADA therefore recognizes thA (**1**) as a valid substrate, corroborating the truly isomorphous nature of this fluorescent nucleoside analogue, and quantitatively converts it to thI (**2**) in about one hour.

The enzyme kinetic parameters V_{max} (5.15 mAbs s⁻¹) and K_{m} (417 μM) of the deamination reactions were determined by Henri-Michaelis-Menten analysis for both thA and A (Figures 4a and 4b, Table 2). The experimental results are alternatively plotted in a Lineweaver-Burk graph (Figures 4c and 4d, Table 2). According to the Henri-Michaelis-Menten kinetics, K_{m} values of 417 and 29 μM are obtained for the thA to thI, and A to I conversion, respectively. The lower conversion rate of thA, compared to that of adenosine, appears to be due to the lower affinity of the former to ADA. We speculate that the higher K_{m} values observed for thA are likely due to the replacement of N⁷ in adenosine with a CH group in thA, as previous structural analysis has shown contacts between side chain residues and this heterocyclic position of the substrate.^[10,16] Nonetheless, as demonstrated below, the performance of thA as a substrate surrogate and the enhanced and distinct emission observed upon its ADA-mediated deamination to thI, provide a robust foundation for a high throughput assay for inhibitor discovery.

To illustrate the prospective for high throughput screening and discovery of novel ADA inhibitors, of particular importance for the treatment of certain leukemias,^[11] we developed a 96-well plate based assay, exploiting the rapid and sensitive fluorescence monitoring of the deamination reaction. The emission enhancement, associated with the conversion of thA (**1**) to thI (**2**) was monitored over a 60-minute time window with increasing concentrations of EHNA and Pentostatin, known ADA inhibitors (Figure 5a). As shown in Figures 5b and 5c, the inhibition of ADA is readily apparent even at low nM concentrations. Guanosine, used as a negative control, had no impact on the deamination reaction up to 100 nM (Figure S5.1).^[14] Despite the relatively rudimentary nature of this high throughput format, the data obtained can be easily quantified. Plotting the percent inhibition at 60 minutes against log[inhibitor] and applying a sigmoidal fit yield IC₅₀ values of 13.4 \pm 1.3, and 1.9 \pm 0.1 nM for EHNA and Pentostatin, respectively, illustrating the established higher potency of the latter. We note that current methods for identifying inhibitors typically rely on either absorption spectroscopy (where other nucleoside-based inhibitory motifs are likely to cause interference) or chromatographic methods, which require relatively large quantities and are not normally amenable for high throughput formats.

To summarize, we have demonstrated the ability of an isomorphous emissive adenosine analogue thA (**1**) to serve as a viable substrate for ADA, a nucleoside-modifying enzyme.^[17] The enzymatic deamination process yields the corresponding emissive inosine analogue thI (**2**), which possesses distinct spectral features, allowing one to monitor the enzyme-catalyzed reaction and its inhibition in real time. To demonstrate its practical utility, we applied this process for the fabrication of a high throughput assay for the discovery and biophysical evaluation of ADA inhibitors, key agents for researchers and clinicians. This

unique proof-of-principle process, where the nucleobase core of a fluorescent nucleoside analogue is enzymatically transformed into a distinctly emissive product, demonstrates a new facet for isomorphous nucleoside analogues and expands their utility landscape beyond their “natural” and typically explored oligonucleotide environments.

Supplementary Material

Refer to Web version on PubMed Central for supplementary material.

Acknowledgments

[**] We thank the National Institutes of Health for support (grant GM 069773) and Dr. Y. Su, Chemistry & Biochemistry, UCSD, for help with the LC-MS experiments.

References

- [1]. a) Sprecher CA, Johnson WC. *Biopolymers*. 1977; 16:2243–2264. [PubMed: 334279] b) Callis PR. *Annu. Rev. Phys. Chem.* 1983; 34:329–357. c) Peon J, Zewail AH. *Chem. Phys. Lett.* 2001; 348:255–262. d) Onidas D, Markovitsi D, Marguet S, Sharonov A, Gustavsson T. *J. Phys. Chem. B*. 2002; 106:11367–11374. e) Cohen B, Crespo-Hernandez CE, Kohler B. *Faraday Discuss.* 2004; 127:137–147. [PubMed: 15471343]
- [2]. Selected reviews: Hawkins ME, Brand L, Johnson ML. *Methods Enzymol.* 2008; 450:201–231. [PubMed: 19152862]; Dodd DW, Hudson RHE. *Mini-Rev. Org. Chem.* 2009; 6:378–391.; Tor Y. *Pure Appl. Chem.* 2009; 81:263–272.; Wilhelmsson LM. *Q. Rev. Biophys.* 2010; 43:159–183. [PubMed: 20478079]; Kimoto M, Cox RSI, Hirao I. *Expert Rev. Mol. Diagn.* 2011; 11:321–331. [PubMed: 21463241]; Sinkeldam RW, Greco NJ, Tor Y. *Chem. Rev.* 2010; 110:2579–2619. [PubMed: 20205430]
- [3]. a) Lakowicz, JR. *Principles of fluorescence spectroscopy*. 3rd ed.. Springer; New York: 2006. b) Valeur, B. *Molecular fluorescence, principles and applications*. Wiley-VCH; Weinheim: 2002.
- [4]. Selected contributions: Ward DC, Reich E, Stryer L. *J. Biol. Chem.* 1969; 244:1228–1237. [PubMed: 5767305]; Greco NJ, Tor Y. *J. Am. Chem. Soc.* 2005; 127:10784–10785. [PubMed: 16076156]. Liu CH, Martin CT. *J. Mol. Biol.* 2001; 308:465–475. [PubMed: 11327781]; Tor Y, Del Valle S, Jaramillo D, Srivatsan SG, Rios A, Weizman H. *Tetrahedron*. 2007; 63:3608–3614.; Srivatsan SG, Greco NJ, Tor Y. *Angew. Chem.* 2008; 120:6763–6767.; *Angew. Chem. Int. Ed. Engl.* 2008; 47:6661–6665. [PubMed: 18683267]; Gaided NB, Glasser N, Ramalanjaona N, Beltz H, Wolff P, Marquet R, Burger A, Mely Y. *Nucleic Acids Res.* 2005; 33:1031–1039. [PubMed: 15718302]. Nadler A, Strohmeier J, Diederichsen U. *Angew. Chem.* 2011; 123:5504–5508.; *Angew. Chem. Int. Ed.* 2011; 50:5392–5396.; Xie Y, Maxson T, Tor Y. *J. Am. Chem. Soc.* 2010; 132:11896–11897. [PubMed: 20690779]; Xie Y, Dix AV, Tor Y. *Chem. Commun.* 2010; 46:5542–5544.
- [5]. a) Caiolfa VR, Gill D, Parola AH. *Biophys. Chem.* 1998; 70:41–56. [PubMed: 9474762] b) Caiolfa VR, Gill D, Parola AH. *FEBS Lett.* 1990; 260:19–22. [PubMed: 2153576] c) Secrist JA, Barrio JR, Leonard NJ. *Science*. 1972; 175:646–647. [PubMed: 4257930] d) Secrist JA, Weber G, Leonard NJ, Barrio JR. *Biochemistry*. 1972; 11:3499–3506. [PubMed: 4340904]
- [6]. a) Haugland R, Johnson I. *J. Fluorescence*. 1993; 3:119–127. b) Lavis LD, Raines RT. *ACS Chem. Biol.* 2008; 3:142–155. [PubMed: 18355003] c) Wysocki LM, Lavis LD. *Curr. Opin. Chem. Biol.* 2011; 15:752–759. [PubMed: 22078994] d) Goddard JP, Reymond JL. *Curr. Opin. Biotechnol.* 2004; 15:314–322. [PubMed: 15358001] e) Reymond J-L, Fluxa VS, Maillard N. *Chem. Commun.* 2009:34–46. f) Rajapakse A, Linder C, Morrison RD, Sarkar U, Leigh ND, Barnes CL, Daniels JS, Gates KS. *Chem. Res. Toxicol.* 2013; 26:555–563. [PubMed: 23488987] g) Razgulin A, Ma N, Rao J. *Chem. Soc. Rev.* 2011; 40:4186–4216. [PubMed: 21552609]
- [7]. a) Adams SR, Tsien RY. *Annu. Rev. Physiol.* 1993; 55:755–784. [PubMed: 8466191] b) Mitchison TJ, Sawin KE, Theriot JA, Gee K, Mallavarapu A. *Methods Enzymol.* 1998; 291:63–78. [PubMed: 9661145] c) Specht A, Bolze F, Omran Z, Nicoud J-F, Goeldner M. *HFSP J.* 2009; 3:255–264. [PubMed: 20119482] d) Li W-H, Zheng G. *Photochem. Photobiol. Sci.* 2012;

- 11:460–471. [PubMed: 22252510] e) Lee H-M, Larson DR, Lawrence DS. *ACS Chem. Biol.* 2009; 4:409–427. [PubMed: 19298086]
- [8]. a) Frederik S. *Arch. Biochem. Biophys.* 1966; 113:383–388. [PubMed: 5941196] b) Baer HP, Drummond GI, Gillis J. *Arch. Biochem. Biophys.* 1968; 123:172–178. [PubMed: 5689048] c) Simon LN, Bauer RJ, Tolman RL, Robins RK. *Biochemistry.* 1970; 9:573–577. [PubMed: 5461216] d) Gillerman I, Fischer B. *J. Med. Chem.* 2011; 54:107–121. [PubMed: 21138280] e) Follmann H, Hogenkamp HPC. *Biochemistry.* 1971; 10:186–192. [PubMed: 5538605] f) Follmann, H. *Nuclear Magnetic Resonance Spectroscopy in Molecular Biology.* Pullman, B., editor. D. Reidel Publishing Company; Dordrecht, Holland: 1978. p. 323–337. g) Leonard NJ. *Crit. Rev. Biochem. Mol. Biol.* 1984; 15:125–199. h) Reinecke D, Schwede F, Genieser H-G, Seifert R. *Plos One.* 2013; 8:1–13.
- [9]. Shin D, Sinkeldam RW, Tor Y. *J. Am. Chem. Soc.* 2011; 133:14912–14915. [PubMed: 21866967]
- [10]. a) Wilson DK, Rudolph FB, Quioco FA. *Science.* 1991; 252:1278–1284. [PubMed: 1925539] b) Kinoshita T, Nakanishi I, Terasaka T, Kuno M, Seki N, Warizaya M, Matsumura H, Inoue T, Takano K, Adachi H, Mori Y, Fujii T. *Biochemistry.* 2005; 44:10562–10569. [PubMed: 16060665] c) Kinoshita T, Nishio N, Nakanishi I, Sato A, Fujii T. *Acta Crystallographica Section D.* 2003; 59:299–303.
- [11]. a) Cristalli G, Costanzi S, Lambertucci C, Lupidi G, Vittori S, Volpini R, Camaioni E. *Med. Res. Rev.* 2001; 21:105–128. [PubMed: 11223861] b) Glazer RI. *Cancer Chemother. Pharmacol.* 1980; 4:227–235. [PubMed: 7002342] c) Odwyer PJ, Wagner B, Leylandjones B, Wittes RE, Cheson BD, Hoth DF. *Ann. Intern. Med.* 1988; 108:733–743. [PubMed: 3282467]
- [12]. Lai TF, Marsh RE. *Acta Crystallogr., Sect. B: Struct. Sci., Cryst. Eng. Mater.* 1972; 28:1982–1989.
- [13]. Thewalt U, Bugg CE, Marsh RE. *Acta Crystallogr., Sect. B: Struct. Sci., Cryst. Eng. Mater.* 1970; 26:1089–1101.
- [14]. See Supporting Information for additional details.
- [15]. Ford H, Dai F, Mu L, Siddiqui MA, Nicklaus MC, Anderson L, Marquez VE, Barchi JJ. *Biochemistry.* 2000; 39:2581–2592. [PubMed: 10704207]
- [16]. Ikehara M, Fukui T. *Biochim. Biophys. Acta.* 1974; 338:512–519.
- [17]. See: Bass BL. *Annu. Rev. Biochem.* 2002; 71:817–846. [PubMed: 12045112] ; Valente L, Nishikura K. *Prog. Nucleic Acid Res. Mol. Biol.* 2005; 79:299–338. [PubMed: 16096031] ; Maas S, Kawahara Y, Tamburro KM, Nishikura K. *RNA Biol.* 2006; 3:1–9. [PubMed: 17114938] ; Maydanovych O, Beal PA. *Chem Rev.* 2006; 106:3397–3411. [PubMed: 16895334] ; Barraud P, Allain FH-T. *Curr. Top. Microbio. Immunol.* 2012; 353:35–60. for reviews of A to I deamination in oligonucleotides (RNA editing), a process mediated by distinct enzymes known as ADARs.

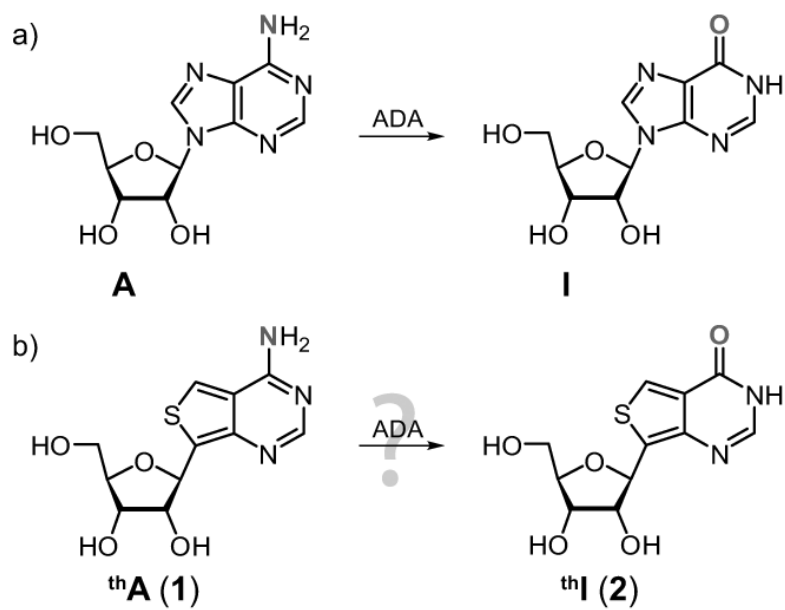


Figure 1.
ADA catalyzed interconversion of a) A to I and b) thA (1) to thI (2).

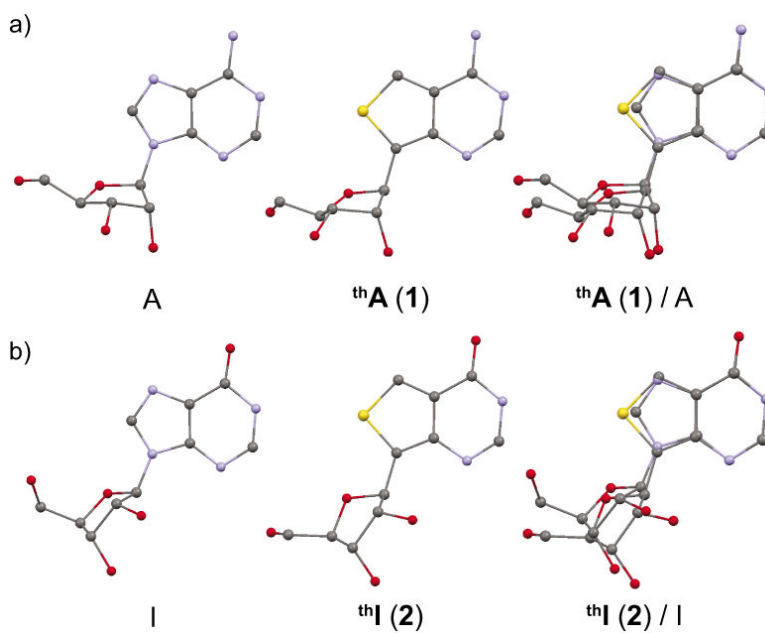


Figure 2. Crystal structures of a) A, thA (1), and their nucleobase overlay (RMS: 0.0383), and b) I, thI(2), and their nucleobase overlay (RMS: 0.0330).^[14]

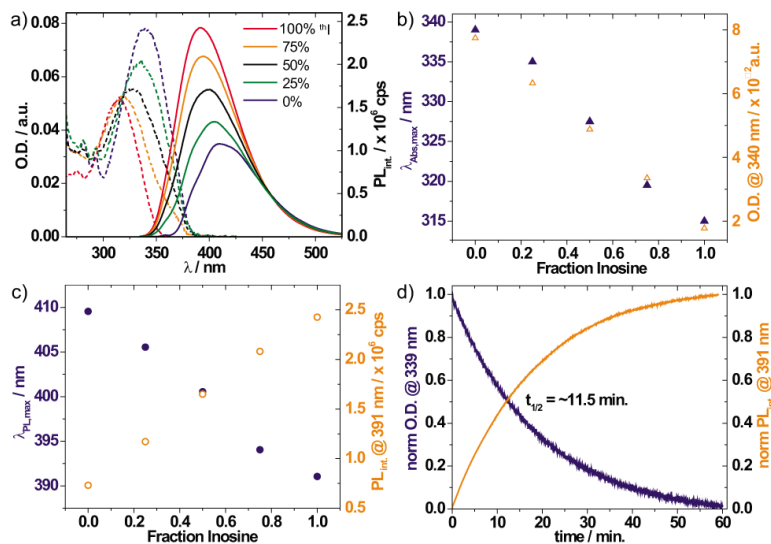


Figure 3.

a) Absorption (dashed lines) and emission (solid lines) spectra of samples prepared with different ratios thA (1) and thI (2) of 11 μM in phosphate buffers of pH 7.4; b) correlation between inosine fraction and λ_{abs,max} (solid blue triangles) and O.D. (open orange triangles) at 340 nm; c) correlation between λ_{em,max} (solid blue circles) and PL_{int} at 391 nm (open orange circles); and d) enzymatic deamination of thA (1) to thI (2) with ADA monitored in real-time by absorption at 339 nm (blue) and emission at 391 nm (orange; excitation at 318 nm). Reaction conditions: [thA] = 11.7 μM, [ADA] = 27 mU/mL in 50 mM phosphate buffer of pH 7.4 kept at 25 °C for 1h. The normalized kinetic curves yield a t_{1/2} of 11.5 min.

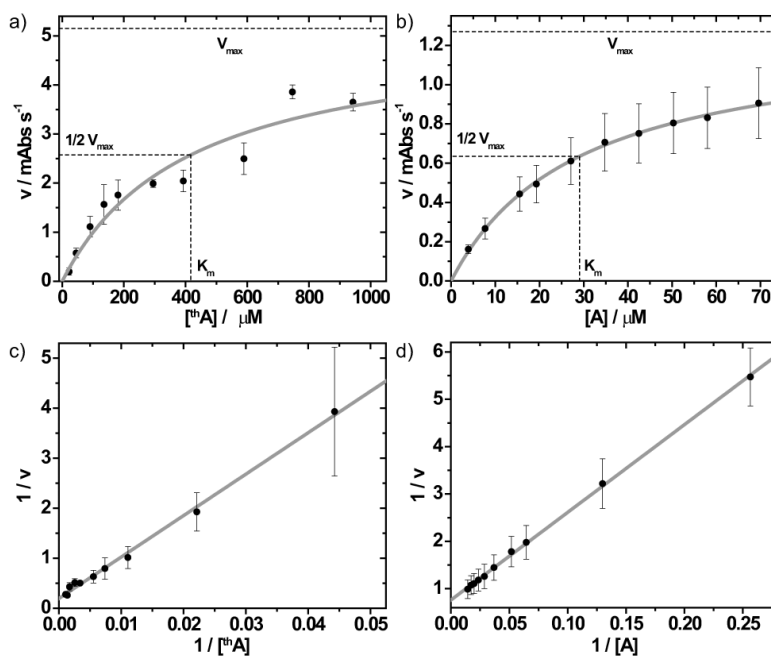


Figure 4. Henri-Michaelis-Menten plots for a) ${}^{\text{th}}\text{A}$ to ${}^{\text{th}}\text{I}$ and b) A to I conversion. Lineweaver-Burk representations are given for c) ${}^{\text{th}}\text{A}$ to ${}^{\text{th}}\text{I}$ and d) A to I conversion. The experiments are performed in triplicate and averaged (solid circles). The error bars reflect the standard error of mean. For panel 4a and 4b the data points are fit to a Hill equation and for panel 4c and 4d the data points are linearized (grey lines). Conditions for a and c): $[{}^{\text{th}}\text{A}] = 22.6 - 942.6 \mu\text{M}$, $[\text{ADA}] = 43.4 \text{ mU/mL}$, and b and d) $[A] = 3.9 - 69.6 \mu\text{M}$, $[\text{ADA}] = 4.1 \text{ mU/mL}$. All experiments are performed in 50 mM phosphate buffer of pH 7.4 at 25 °C.

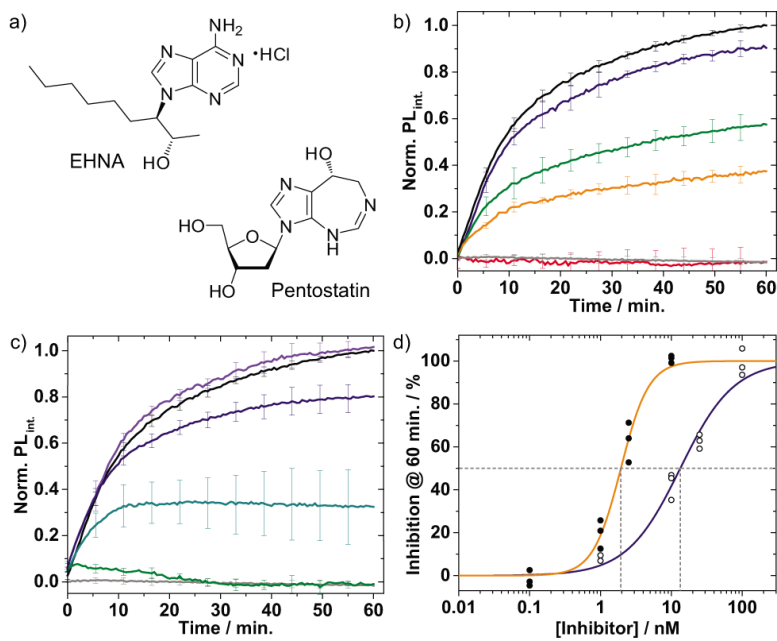
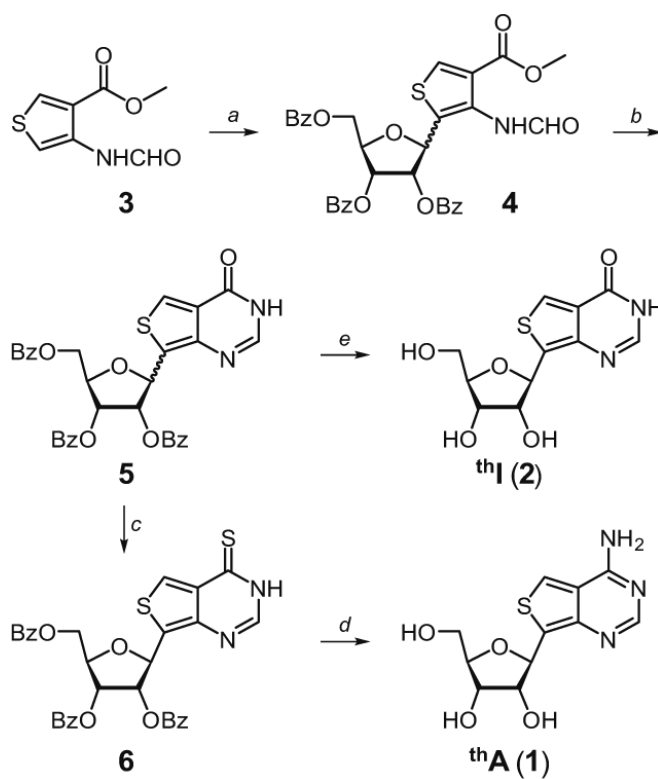


Figure 5.

a) Structures of ADA inhibitors EHNA and Pentostatin; conversion of thA (**1**) followed with fluorescence in the presence of b) EHNA and c) Pentostatin (black, purple, blue, cyan, green, orange, and red lines represent 0, 0.1, 1, 2.5, 10, 25, 100 nM [inhibitor], respectively. The grey lines represent the conversion of thA (**1**) in the absence of ADA. The experiment is performed in triplicate and error bars reflect the standard deviation. d) A plot of % inhibition at 60 min. vs. log[inhibitor] in triplicate (data points) and sigmoidal logistic fits performed in OriginPro (lines) for EHNA (open circles, blue line, R^2 :0.97155) and Pentostatin (solid circles, orange line, R^2 :0.98437). The grey dashed lines visualize graphical determination of the IC₅₀ values. Actual values have been interpolated using the fit. Assay conditions: [thA] = 11.7 μ M, [ADA] = 27 mU/mL, in 50 mM phosphate buffer of pH 7.4 at 21 $^{\circ}$ C.

**Scheme 1.**

Synthesis of **thA (1)** and **thI (2)**. *Reagents and conditions:* (a) β -D-ribofuranose 1-acetate 2,4,5-tribenzoate, SnCl_4 , MeNO_2 , 65°C , 32%; (b) (i) 15% HCl (aq.) in MeOH , CHCl_3 , quantitative; (ii) formamidine \cdot AcOH, EtOH , Δ , α -21%, β -39%; (c) P_2S_5 , Py , 43%; (d) NH_3/MeOH , 100°C , 86%; (e) NH_3/MeOH , 45°C , 17h (86%).

Table 1Relevant spectroscopic properties of thA (**1**) and thI (**2**)^a.

	$\lambda_{\text{abs.max.}}$	ϵ	rel. Abs _{int.} @ 339 nm	$\lambda_{\text{em.max.}}$	rel. PL _{int.} @ 391 nm
th A (1)	339	7.1×10^3	3.9	410	1.0
th I (2)	315	4.8×10^3	1.0	391	3.3

^a λ , and ϵ are reported in nm and $\text{M}^{-1}\text{cm}^{-1}$, respectively.

Table 2Enzyme parameters for the deamination of thA (**1**) and adenosine^a.

	Henri-Michaelis-Menten			Lineweaver-Burk		
	V_{\max}	K_m	R^2	V_{\max}	K_m	R^2
th A to th I	5.15	417	0.91247	5.07	420	0.99530
A to I	13.4 ^[b]	29	0.99832	14.0 ^[b]	24	0.99924

^[a] V_{\max} , and K_M are reported in mabs/s, and μM , respectively.

^[b] V_{\max} is linearly dependent on [ADA]. To correct for the 10.58 fold lower [ADA] used in the A to I experiment, the apparent V_{\max} (1.27 and 1.32 mabs/s), obtained from Fig. 4b and 4d, respectively, is multiplied by 10.58.